



Assessment of Particle-size and Temperature Effect of Nanofluid on Heat Transfer Adopting Lattice Boltzmann Model

A. Shahriari^a, N. Jahantigh^{*a}, F. Rakani^b

^aDepartment of Mechanical Engineering, University of Zabol, Zabol, Iran

^bDepartment of Computer Sciences, University of Sistan & Baluchestan, Zahedan, Iran

PAPER INFO

Paper history:

Received 18 November 2017

Received in revised form 08 December 2017

Accepted 05 February 2018

Keywords:

Nanoparticles Mean Diameter

Natural Convection

Nanofluid

Lattice Boltzmann Model

ABSTRACT

The investigation of the effect of nanoparticles' mean diameter and temperature of Al₂O₃-water nanofluid on velocity and energy field using the lattice Boltzmann method is the main objective of this study. The temperature of the vertical walls is considered constant at T_c and T_h, respectively, while the up and the down horizontal surfaces are smooth and insulated against heat and mass. The influences of Grashof number (10³, 10⁴, 10⁵) Prandtl number (Pr=3.42, 5.83), the various volume fraction of nanoparticles (φ=0, 0.01, 0.03, 0.05) and particle-size (d_p= 24, 47, 100 nm) were carried out on heat transfer and flow fields. It was concluded that addition of nanoparticles causes a significantly affect on temperature and flow fields. The decrement of heat transfer is observed with the increment of solid volume fraction, but it increases when Grashof number and nanoparticles' mean diameter increase. The decrement of nanoparticles' mean diameter and Prandtl number have the same effect on Nusselt number. In addition, it was resulted that the thermal conductivity model had insignificantly impact on the mean Nusselt number than the dynamic viscosity model.

doi: 10.5829/ije.2018.31.10a.18

1. INTRODUCTION

The laminar free convective heat transfer plays an important role in engineering science and industrial field. It has many thermal and engineering applications like furnaces, double pane windows, heat exchangers, cooling and heating building, solar technology, structure insulating, cooling of electronic instruments, etc. [1].

Calgagni et al. [2] and Kuznik et al. [3] have investigated the free convective heat transfer within an enclosure in various studies.

The performance of systems with basic operation fluid for instance water, types of oils do not increase because their thermal conductivity is low and these fluids do not have compactness capability. Choi has presented a new technique to improve heat transfer which uses dispersion solid particles in the nanoscale dimension (size <100nm) in a thermal system with a base fluid [4].

The clogging in micro channels does not occur in systems that the mixture of fluid and nanoparticles is used because of unique physical and chemical properties including low sedimentation, high thermal conductivity and stability in comparison with particles having millimeter or micrometer size.

Study on nano-fluids is in high interests duo to their properties and other benefits for example pumping reduction, homogeneity, and long-term stability [5].

The effect of Brownian motion on natural convection, simulation and prediction of dissipative nanofluid flow as well as similarity solution for mixed-convection boundary layer nanofluid flow were reported in literature [6-8].

Murshed et al. [9], Choi et al. [10], and Khanafer et al. [11] have demonstrated the behavior of solid particles in cavity is similar to liquid molecules having large specific surface areas nanoparticles because of very small sizes. The natural convection heat transfer was experimentally investigated on different nano fluids by Putra et al. [12] and Wen and Ding [13]. They found

*Corresponding Author Email: njahantigh@uoz.ac.ir (N. Jahantigh)

that the natural convection heat transfer does not increase with increment of the nanoparticles concentration. The thermal parameters of free convection within an enclosure including Al_2O_3 - water nanofluid has studied theoretically by Hwang et al. [14]. They applied various models to calculate dynamic viscosity. Also, they used the empirical relations to estimate the coefficient of the nanofluid heat transfer. They found that nanoparticles had adverse effects on heat transfer in the free convection regime. As shown in the diagrams of coefficient of heat transfer and Nusselt number correlation, the Nu number increases along with increment of the nanoparticles' average diameter or decrement the nanofluid temperature. Kim et al. [15] studied the convection instability of free convection nanofluid through RB regime analytically and observed a similar process. The convective heat transfer coefficient has increased because of the presence of solid particles. Khanafer et al. [11] has studied the heat transfer within an enclosure, which heated differentially including Copper nanoparticle numerically while Gr varying between 10^3 to 10^5 . They observed that the rate of heat transfer has raised due to increasing of the suspended nanoparticles percentage through the various Gr number. Lin and Violi [16] have examined the free convection regime in a vertical enclosure including Alumina nanoparticle containing different volume fractions, Grashof and Prandtl numbers and nanoparticles' mean diameter numerically. They adopted the presented model by Jang et al. [17] toward define the effective viscosity (the temperature is not effective in this model) and also the model presented by Xu et al. [18] for determination of the effective thermal conductivity. They indicated that the heat transfer parameters of the nanofluid can be increased as the particle's sized is reduced from 250 to 5 nm. Moreover, the augment of mixture temperature causes to enhance the effect of nanoparticles' mean diameter inside the cavity. They found a direct relation between Nusselt number and nanoparticle volume fraction increase for constant nanoparticles' mean diameter and temperature, which is in contrast with experimental data reported in literature [19, 20].

It was concluded that the dynamic viscosity of nanofluid depends on the nanoparticles' mean diameter and the nanofluid temperature Nguyen et al. [19], Li et al. [20], and Masoumi et al. [21]. The natural convection of nanofluids articles have not been studied the impact of temperature in effective dynamic viscosity models.

In recent years, due to advantages of numerical methods including LBM such as simplicity of programming, possibility of parallel computation, and easy application of boundary conditions have been used extensively.

To the best knowledge of the researchers here, there is not any available papers that considered LBM method to investigate the impacts of nanoparticles mean diameter and temperature of nanofluid on the flow and heat transfer parameters. Thus, in this study, some models are adopted to determine the nanofluid dynamic viscosity and thermal conductivity. Masoumi [21] model is applied to calculate the effective dynamic viscosity and the Chon [22] model is used to define the thermal conductivity. These models include both effects of the nanoparticles' mean diameter and nanofluid temperature that are based on the experimental measurements. In this study, the effects of pertinent parameters for instance Gr and Prandtl numbers and solid particle volume fraction on the nanofluid heat transfer characteristic insight an enclosure were investigated.

2. PROBLEM STATEMENT

The geometry of a square enclosure with the size of $W \times H$ applied in computational area is displayed schematically in Figure 1. It is observed from Figure 1 that the right and left vertical surfaces are flat and heated at the temperature T_c and T_h , respectively. The horizontal top and bottom smooth surfaces are insulated against heat and mass. Nanofluid within the cavity is initially at rest (particle volume fraction can fluctuate as $0 \leq \phi \leq 5\%$). Next, the temperature difference between left and right walls causes a buoyancy force and fluid motion. In addition, the variation of density is insignificant thus; Boussinesq approximation is used to coupling velocity and thermal fields equations.

In the present study, the flow of a nanofluid which consists of water and aluminum oxide nanoparticles is subjected to the assumptions of incompressible, single-phase, no-chemical reaction, no-slipage between water and solid nanoparticles, negligible thermal radiation and viscous dissipation due to its small effects. Also, it is supposed that the flow to be laminar and steady. The physical and thermal properties of water and aluminum oxide particles were tabulated in Table 1.

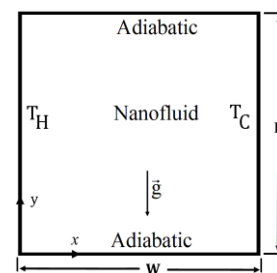


Figure 1. Graphical representation of the system under consideration

TABLE 1. properties of the water and aluminum oxide particles

Properties	H ₂ O	Aluminium Oxide
C _p (J/kgK)	4179	765
ρ (kg/m ³)	997.1	3970
k (W/mK)	0.613	25
β×10 ⁵ (1/K)	21	0.85
dp (nm)	0.384	24.47 and 100

The value of Prandtl numbers were 5.83 and 3.42 for temperatures of 300⁰K and 325⁰K, respectively. The variations of alumina nanofluid physical and thermal properties are negligible with respect the temperature, except in Boussinesq approximation.

3. NUMERICAL APPROACH

Here a discussion about thermal lattice Boltzmann method is presented due to its relevant to the present study. Thermal LMB uses of the distribution function f_i for velocity field and distribution functions g_i for energy field. A standard two-dimensional nine-velocity called D2Q9 lattice Boltzmann method with Bhatnagar–Gross–Krook approximation is employed for the flow field, in the computational domain here as shown in Figure 2.

For the evolution of velocity field, the LB equation can be discretized as following [23]:

$$f_i(\vec{x} + \vec{c}_i\Delta t, t + \Delta t) = f_i(\vec{x}, t) + \frac{\Delta t}{\tau_\theta} \cdot [f_i^{eq}(\vec{x}, t) - f_i(\vec{x}, t)] \tag{1}$$

Here, f_i and f_i^{eq} are functions for particle and equilibrium distributions along with direction, respectively. c_i is discrete velocity vector for a moving pseudo-particle which that for the D2Q9 lattice model is computed as:

$$c_i = \begin{cases} 0 & ; i = 0 \\ 1 & ; i = 1 - 4 \\ \sqrt{2} & ; i = 5 - 8 \end{cases} \tag{2}$$

The local equilibrium distribution functions f_i^{eq} are given in reference [23]:

$$f_i^{eq} = \omega_i \rho \left[1 + \frac{9(\vec{c}_i \cdot \vec{u})^2}{2c^4} - \frac{3\vec{u}^2}{2c^2} + 3\frac{\vec{c}_i \cdot \vec{u}}{c^2} \right] \tag{3}$$

where, u is macroscopic velocity and ρ is the fluid density. The ω_i are weight coefficients as follow:

$$\omega_i = \begin{cases} 4/9 & i = 0 \\ 1/9 & i = 1 - 4 \\ 1/36 & i = 5 - 8 \end{cases} \tag{4}$$

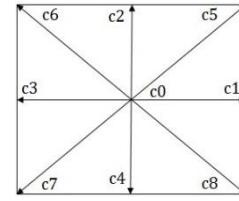


Figure 2. D2Q9 lattice

Chapman–Enskog analysis can be applied to recover Navier–Stokes equation from the LB equation. As a result, the single relaxation time and viscosity ϑ are related to each other as:

$$\vartheta = c_s^2 \Delta t (\tau_\theta - 0.5) \tag{5}$$

The positivity of the kinetic viscosity requires $\tau_\theta > 0.5$. Macroscopic flow mass density and momentum variables can be calculated through the following relations, respectively [23].

$$\rho = \sum_{i=0}^8 f_i \tag{6}$$

$$\rho \vec{u} = \sum_{i=0}^8 \vec{c}_i f_i \tag{7}$$

where, ρ and u are the lattice fluid density and velocity, respectively.

The particle density distribution function given in Equation (3) is solved by two computational steps of collision and propagation. These two steps can be formulated as Equations (8) and (9), respectively [23]:

$$\tilde{f}_i(\vec{x}, t + \Delta t) = f_i(\vec{x}, t) - \frac{\Delta t}{\tau_\theta} [f_i(\vec{x}, t) - f_i^{eq}(\vec{x}, t)] \tag{8}$$

$$f_i(\vec{x} + \vec{c}_i\Delta t, t + \Delta t) = \tilde{f}_i(\vec{x}, t + \Delta t) \tag{9}$$

In which, \tilde{f}_i are post-collision particle distribution functions.

The buoyancy body force plays a significant role as an external force in the present study. One of the most widely used methods for introducing the body force term in LBM is its addition to collision operator as [23]:

$$f_i(\vec{x} + \vec{c}_i\Delta t, t + \Delta t) = f_i(\vec{x}, t) - \frac{\Delta t}{\tau_\theta} \cdot [f_i(\vec{x}, t) - f_i^{eq}(\vec{x}, t)] + \Delta t F_i(\vec{x}, t) \tag{10}$$

where F_i are the external force term in direction i . Using Boussinesq approximation, it can be expressed by [23]:

$$F_i(\vec{x}, t) = 3\omega_i g_y \beta [T(\vec{x}, t) - T_\infty] \rho(\vec{x}, t) \vec{c}_i \tag{11}$$

where T_∞ and β are reference temperature and thermal expansion coefficient, respectively.

For temperature field by neglecting terms of the viscous dissipation and compressive heating effects, the evolution of temperature distribution function is considered as follows [23]:

$$g_i(\vec{x} + \vec{c}_i \Delta t, t + \Delta t) = g_i(\vec{x}, t) - \frac{\Delta t}{\tau_T} \cdot [g_i(\vec{x}, t) - g_i^{eq}(\vec{x}, t)] \quad (12)$$

In which g_i are temperature distribution functions of the particles in i th direction and τ_T denotes the dimensionless relaxation time. In addition, g^{eq} are the local equilibrium energy distribution functions and for D_2Q_9 model is written by [23]:

$$g_i^{eq} = \omega_i T \left[1 + 3 \frac{\vec{c}_i \cdot \vec{u}}{C^2} + \frac{9}{2} \frac{(\vec{c}_i \cdot \vec{u})^2}{C^4} - \frac{3 \vec{u}^2}{2 C^2} \right] \quad (13)$$

The macroscopic temperature is then defined as following [23]:

$$T = \sum_{i=0}^8 g_i \quad (14)$$

Finally, the thermal diffusivity is rewritten as:

$$\alpha = c_s^2 \Delta t (\tau_T - 0.5) \quad (15)$$

Note that the positivity of the thermal diffusivity needs $\tau_T > 0.5$.

Boundary conditions utilized in the computational domain are expressed in non-dimensional form by:

$$\begin{aligned} U = V = 0, \quad \theta = 1, \quad \text{On the left} \\ U = V = 0, \quad \theta = 0, \quad \text{On the right wall} \\ U = V = 0, \quad \frac{\partial \theta}{\partial y} = 0, \quad \text{On the top and bottom} \end{aligned} \quad (16)$$

Where nondimensional temperature can be defined by:

$$\theta = \frac{T - T_c}{\Delta T} \quad (17)$$

Implementation of boundary conditions in the LBM is an important step in flow simulation as f and g indicating to the computational domain in the boundaries nodes are unknown. The upper and lower solid boundaries are considered as adiabatic which are represented with the bounce back boundary condition. It indicates that the incoming boundary populations towards the solid boundaries bounce back towards computational area. As an illustration at the top wall, the following conditions applied as:

$$f_{4,n} = f_{4,n-1}, \quad f_{7,n} = f_{7,n-1}, \quad f_{8,n} = f_{8,n-1} \quad (18)$$

$$g_{4,n} = g_{4,n-1}, \quad g_{7,n} = g_{7,n-1}, \quad g_{8,n} = g_{8,n-1} \quad (19)$$

Temperatures of vertical smooth surfaces are known ($\theta_{Left}=1, \theta_{Right}=0$), due to utilizing $D2Q9$ scheme, the unknown functions f and g can be specified as the following conditions:

$$f_{3,n} = f_{1,n}, \quad f_{6,n} = f_{8,n}, \quad f_{7,n} = f_{5,n} \quad (20)$$

$$g_{3,n} = -g_{1,n}, \quad g_{6,n} = -g_{8,n}, \quad g_{7,n} = -g_{5,n} \quad (21)$$

Here, subscript n stands for the node on the boundary.

Prandtl and Grashof numbers are the main control variables, which expressed as:

$$Gr = \frac{g_y \beta H^3 \Delta T}{\vartheta_f^2} \quad (22)$$

$$Pr = \frac{\vartheta_f}{\alpha_f} \quad (23)$$

As described earlier, the Al_2O_3 -water is supposed as a single phase media, thus addition of nanoparticles to water has significant effects on thermo-physical properties of the nanofluid. The nanofluid effective properties such $\rho_{nf}, (c_p)_{nf}, \beta_{nf}$ are presented as:

$$\rho_{nf} = (1 - \varphi)\rho_f + \varphi\rho_p \quad (24)$$

$$(\rho c_p)_{nf} = (\rho c_p)_f (1 - \varphi) + (\rho c_p)_p \varphi \quad (25)$$

$$(\rho \beta)_{nf} = (\rho \beta)_f (1 - \varphi) + (\rho \beta)_p \varphi \beta_f \quad (26)$$

where solid nanoparticles, nanofluid and base fluid are respectively defined by subscripts p, nf and f .

The effective nanofluid viscosity is calculated by Equation (27) is developed by Masoumi et al. [21], which is a semi experimental model as:

$$\mu_{nf} = \mu_f + \mu_{app} \quad (27)$$

This model has the close behavior to experimental data and considers the effect of nanoparticles Brownian motion and induced surrounding fluid motion. The μ_{nf} in Equation (27) can be obtained through the apparent viscosity, μ_{app} . It is worth noting that, μ_{app} takes into account the influence of the temperature, mean nanoparticle size and nanoparticle concentration variables.

The results obtained through Equation (27) will be compared to the one proposed by Brinkman [24], expressed as follows:

$$\mu_{nf} = \frac{\mu_f}{(1 - \varphi)^{2.5}} \quad (28)$$

The Chon et al. [22] correlation is applied for calculation k_{nf} as following:

$$\frac{k_{nf}}{k_f} = 1 + 64.7 \varphi^{0.7460} Re^{1.2321} \cdot \left(\frac{d_f}{d_p} \right)^{0.3690} \left(\frac{k_p}{k_f} \right)^{0.7476} Pr_T^{0.9955} Re^{1.2321} \quad (29)$$

Here $Pr_T = \frac{\mu_f}{\rho_f \alpha_f}$ and Re is defined by:

$$Re = \frac{\rho_f K_b T}{3 \pi \mu_f^2 l_f} \quad (30)$$

where, K_b is Boltzmann constant and T is alumina nanofluid temperature, respectively. The value of mean free path (l_f) for water is applied as $l_f = 0.17$ nm.

The viscosity of water is calculated with the relations presented by Fox et al. [25] which is a function of temperature as:

$$\mu_f = a \cdot 10^{b/(T-C)} \tag{31}$$

where

$$a = 2.414 \times 10^{-5}, b = 247.8, c = 140 \tag{32}$$

The dimensionless form of used variables in this paper is as following:

$$U = \frac{uH}{\alpha_f}, V = \frac{vH}{\alpha_f}, X = \frac{x}{W}, Y = \frac{y}{H} \tag{33}$$

$$\alpha = \frac{\alpha_{nf}}{\alpha_f}, \mu = \frac{\mu_{nf}}{\mu_f}, k = \frac{k_{nf}}{k_f},$$

The mean Nusselt numbers according to [23], is:

$$Nu = 1 + \frac{\langle u_x \cdot T \rangle}{\alpha \cdot \Delta T / H} \tag{34}$$

Here, $\langle u_x \cdot T \rangle$ denote the mean value of $(u_x \cdot T)$ in whole computational domain.

4. VALIDATION

As a first step in a computational method, it is required to have results that are not depended on grid size. To this end, as is observed in Figure 3, six mesh sizes are used and mean Nusselt number, Nu_{avg} , at $Ra = 10^4$ for various grid sizes is calculated. It is found from this table that a grid independent solution is obtained with a grid size of at least **161 * 161** points. Hence, a grid size of **161 * 161** points is used in all computations to compromise between computational cost and accuracy. The computational convergence criterion applied in this study, is defined as:

$$\epsilon = \frac{\sum_{i=1}^n \sum_{j=1}^m |T^{n+1} - T^n|}{\sum_{i=1}^n \sum_{j=1}^m |T^n|} < 10^{-8} \tag{35}$$

Here, n denotes the iteration number and ϵ is the tolerance.

The present numerical solution has been validated through published papers in the literature. The Nu_{avg} on left wall for different Ra the square cavity is shown in Table 2 with those of other numerical investigations. Good correspondence is observed between present computations and previous works. In addition, comparison of temperature distribution in the middle of the square enclosure with those reported in the literature shows good agreement, as is observed in Figure 4.

5. RESULTS

In this part, the influences of different parameters on the hydrodynamic and thermal behavior of nanofluid in a square enclosure are investigated. As mentioned before, the range of volume concentrations is $0 \leq \phi \leq 5\%$ and Grashof number is $Gr=10^3-10^5$. The nanoparticles used

in this investigation are of type Al_2O_3 while keeping Prandtl numbers of the base fluid to 5.83 and 3.42 for temperatures of 300 ^0K and 325 ^0K , respectively.

To make better understanding of the effect of ϕ on flow behavior inside the cavity, typical profiles for U at the mid-section of the square enclosure for $Gr=10^4$, $Pr=5.83$ and mean diameters of 24 and 47 nm are presented in Figure 5. It is clearly seen that for both mean diameters, the maximum velocity peaks seen in the absence of Al_2O_3 nanoparticles. Furthermore, by rising the volume concentration, the magnitude of velocity components decline, where this phenomenon can be explained as the effect of increment of the effective nanofluid viscosity based on Equation (27).

TABLE 2. Comparison of the Nu_{AVG} on hot wall for a system containing pure fluid with $Pr=0.7$

Rayleigh number				Study
10^6	10^5	10^4	10^3	
8.714	4.480	2.238	1.119	Present study
8.799	4.519	2.243	1.118	Davis [28]
8.826	4.522	2.245	1.118	Khanafer et al. [11]
8.976	4.598	2.254	1.117	Wan et al. [13]

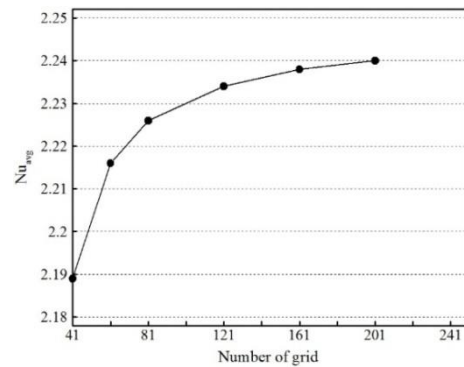


Figure 3. Grid dependency at $Ra = 10^4$ and $Pr=0.7$

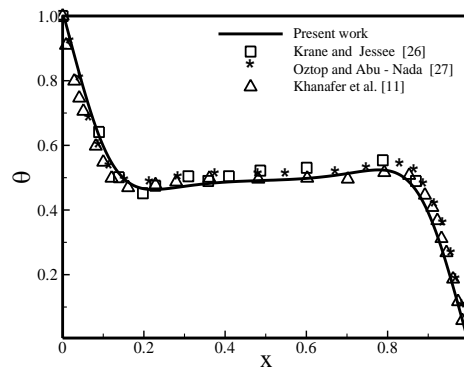


Figure 4. Comparing nondimensional temperature at the vertical mid plan ($Ra=10^5$, $Pr = 0.7$)

Moreover, when the nanoparticle' mean diameter enhances, the influence volume concentration inside the cavity declines.

It is noted that influence of the volume concentration is less pronounced at the center part of cavity where there is a low level of velocity magnitude.

As observed in Figures 6a and 6b the increment of volume concentration causes to decrement the heat transfer rate. This can be explained as follows: when nanoparticles are added, both of μ_{nf} and k_{nf} were increased. However, the incremental effect of μ_{nf} compared to incremental effect of the k_{nf} is dominated at $\phi > 0.0$. Thus, the thermal boundary layer thickness is raised, therefore mean Nusselt number decreases for all Grashof numbers. A good consistency between present result and experimental findings reported in literature [12, 13] who showed that the Nu_{avg} drops by increasing volume concentration.

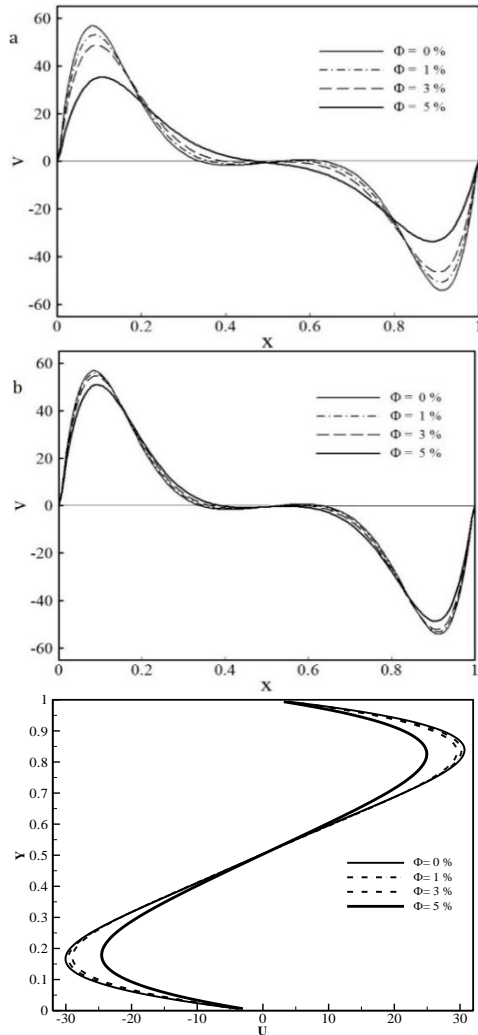


Figure 5. Variation of y-component velocity V and x-component velocity U at mid-section for Pr=5.83, Gr = 10⁴, a) dp = 24 nm, b) dp = 47 nm, c) dp = 24 nm

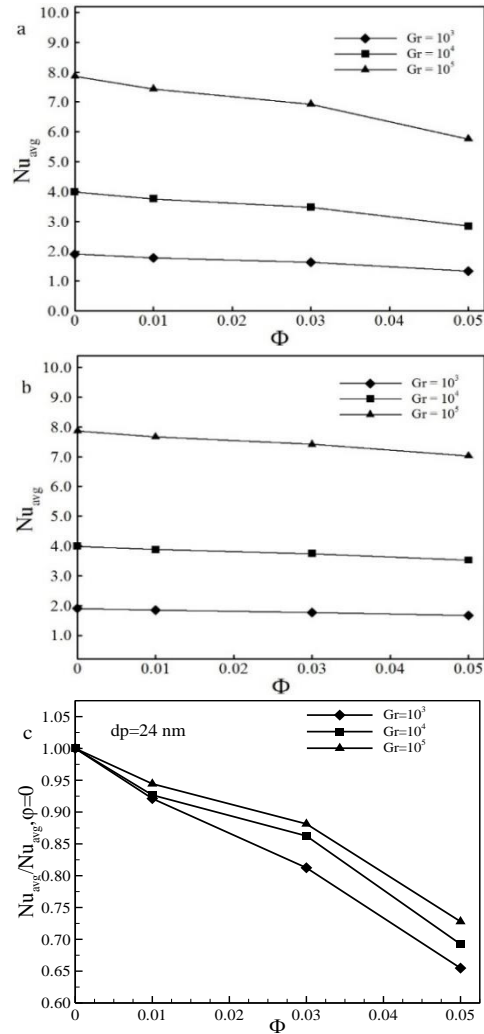


Figure 6. Variation of the Nu_{avg} and Nusselt number ratio at different ϕ and Gr for Pr = 5.83, a) dp = 24 nm, b) dp = 47 nm, c) dp = 24 nm

It can be interesting to note that Nu_{avg} drops significantly for $Gr=10^3$, whereas the trend slows at other Grashof number (see Figure 6c).

To study latter effect on the nanoparticles' size has to fluctuate among 24 to 100 nm and the Prandtl number and volume concentration are kept constant at 5.83 and 0.05, respectively. The vertical velocity profile at the midsection is affected by different nanoparticles' mean diameter is observed in Figure 7. Where, the nanoparticles' mean diameter increment leads to increase the maximum velocity profile and the heat transfer. This behavior is similar to volume concentration reduction. In other words, declining of nanoparticles' mean diameter and increasing of the volume concentration have the same effect. The dominate influence of dynamics' viscosity on the characteristic of heat transfer nanofluid is a major cause of this phenomena.

Figure 8 shows Nusselt number distribution for different volume concentration at $Pr = 5.83$, nanoparticles' mean diameters $dp= 24, 47, 100$ nm and Grashof numbers of 10^3 and 10^4 .

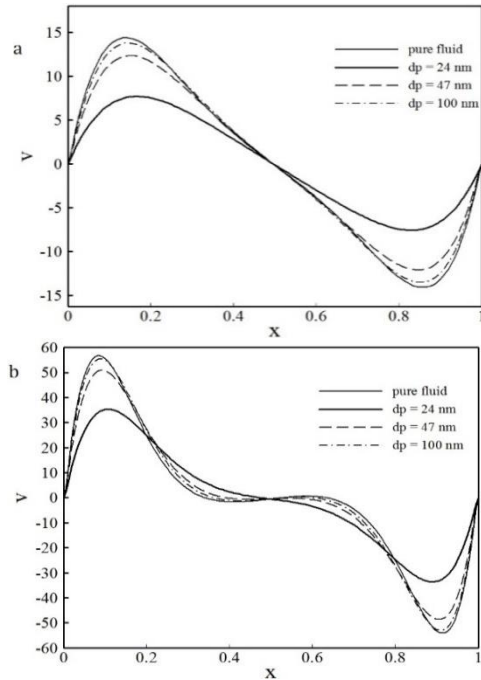


Figure 7. Variation of y-component velocity V at mid-section for $Pr = 5.83, \phi = 0.05$, a) $Gr = 10^3$, b) $Gr = 10^4$

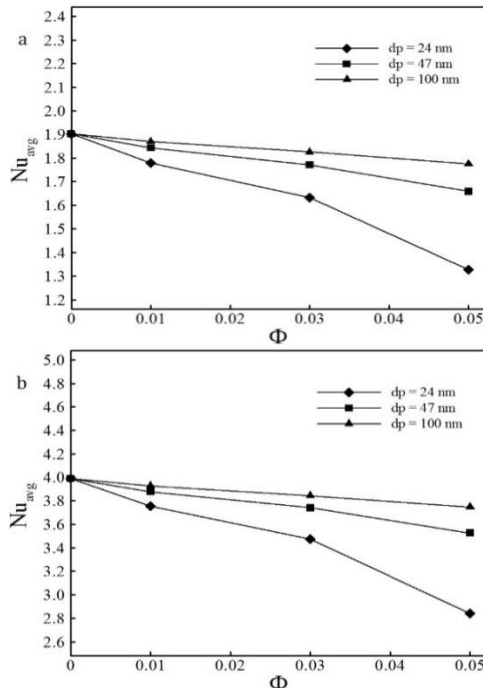


Figure 8. Variation of Nu_{avg} for different ϕ at $Pr = 5.83$, a) $Gr = 10^3$, b) $Gr = 10^4$

The mean Nusselt number illustrates that heat transfer increases by rising the nanoparticles' mean diameters for various Grashof number and volume concentration, where a similar manner observed by Hwang et al. [14]. In addition, it is obvious that the rate of this decrease is different for various values of nanoparticles' mean diameter, where this reduction trend slows down with the growth of mean diameter.

Streamlines and isotherms for nanofluids and base fluid at $Gr=10^3$ and $Gr=10^5$, for $\phi=0.05$ and $Pr=5.83$, respectively are presented in Figure 9.

Here streamlines patterns described by a small central vortex for $Gr=10^3$ and, the core region of the cavity tends to break up into two recirculation zones for $Gr=10^5$. For $Gr=10^3$ the value of the absolute circulation strength increases as the nanoparticles mean diameter increases. For example, $|\psi|_{max}=2.378$ for 24 nm, whereas it is 3.964 for $dp = 100$ nm (Figure 9). The reason for this is a drop in the nanoparticles' mean diameter and y-component velocity. A similar trend is observed for $Gr=10^5$. However, the variation rate for $Gr=10^5$ is low.

Moreover, for a specific nanoparticles' mean diameter the isotherm diagrams are similar and the variation of Grashof number has no significant effect on them.

The effects of nanofluid temperature are given in term of Prandtl number. The comparing of the isotherms and streamlines contours for Prandtl numbers 5.83 and 3.42 at the $dp = 24, 47$ and 100 nm are shown in Figure 10.

The value of the absolute circulation strength rises as the Pr increases. This reason of this increment is simultaneous changes of the dynamic viscosity and the thermal conductivity, which have temperature dependence. Increasing of Pr has the same effect on streamline and isotherms contours at different nanoparticles' mean diameter, as is observed in Figure 10.

Figure 11 shows that Nusselt number is strongly affected due to changing the Pr and it enhances with a rise of Pr for different values of nanoparticles' mean diameter

Figure 12 presents comprising of various correlations for prediction of μ_{nf} and k_{nf} . The dynamic viscosity ratios are calculated in accordance with Masoumi et al. [21] and Brinkman [24] models as functions of volume concentration ϕ for Prandtl number 5.83 and various nanoparticles' mean diameter. At Figure 12, as the volume fraction augments, difference between the results obtained from Equations (18) and (19) increases, especially at small nanoparticles' mean diameter. For example, for the mean diameter of 24 nm and $\phi=0.01$ to 0.05, the viscosity difference is 11.49% and 54.15 %, whereas for mean diameter of 47 nm and $\phi=0$ to 0.04 it's 2.41% and 10.8%, respectively. In addition, there is a variation in the thermal conductivity

for different temperatures and the nanoparticles' mean diameter, which is also important in this regards as observed in Figures 12b and 12c.

Moreover, the Nusselt number is affected by different dynamic viscosity models as well. As an example, for diameter is increased from 24 to 47 nm, the difference for the Nusselt number is 0.64%. According to Brinkman [24] model and this difference is thoroughly sensitive in Chon et al. [22] model to different nanoparticles' mean diameter. However, for

the last case, the difference in Nusselt number is 7.82% according to Masoumi et al. [21] model. It is obvious that that Brinkman [24] model has no sensitivity to the nanoparticles' mean diameter.

This is due to the Brinkman [24] model does not depend on the nanoparticles' mean diameter. While, the Masoumi et al. [21] model considers the influences of particle density, particles size and temperature. Hence this model can be predicted a more realistic behavior of nanofluid for different parameters.

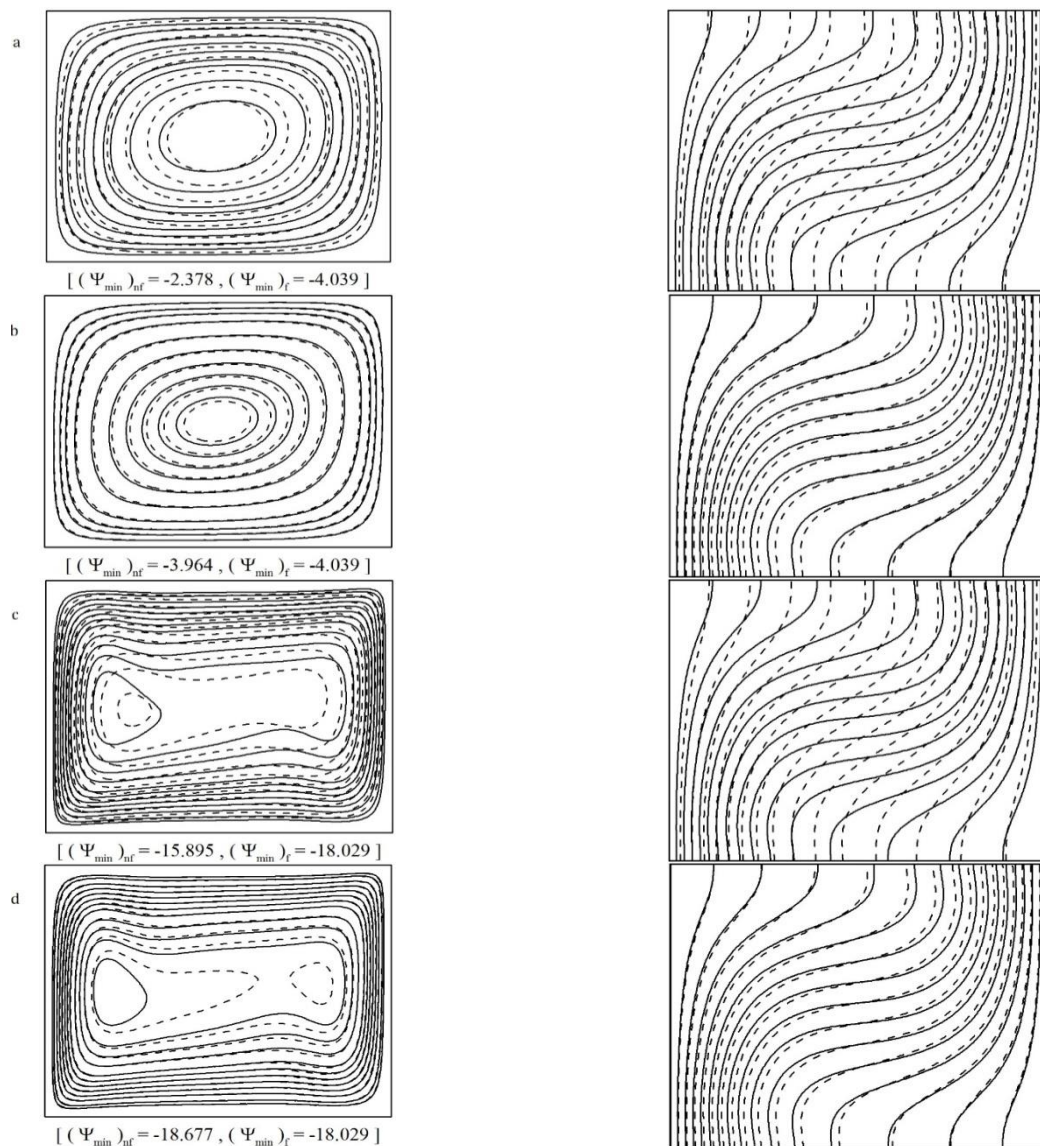


Figure 9. Comparison of the streamlines contours (left) and isotherms contours (right) for pure water (solid line) and nanofluid with $\phi = 0.05$ (dashed line) at $Pr=5.83$ a) $dp=24$ nm, $Gr=10^3$, b) $dp=100$ nm, $Gr=10^3$, c) $dp=24$ nm, $Gr=10^5$, d) $dp=100$ nm, $Gr=10^5$

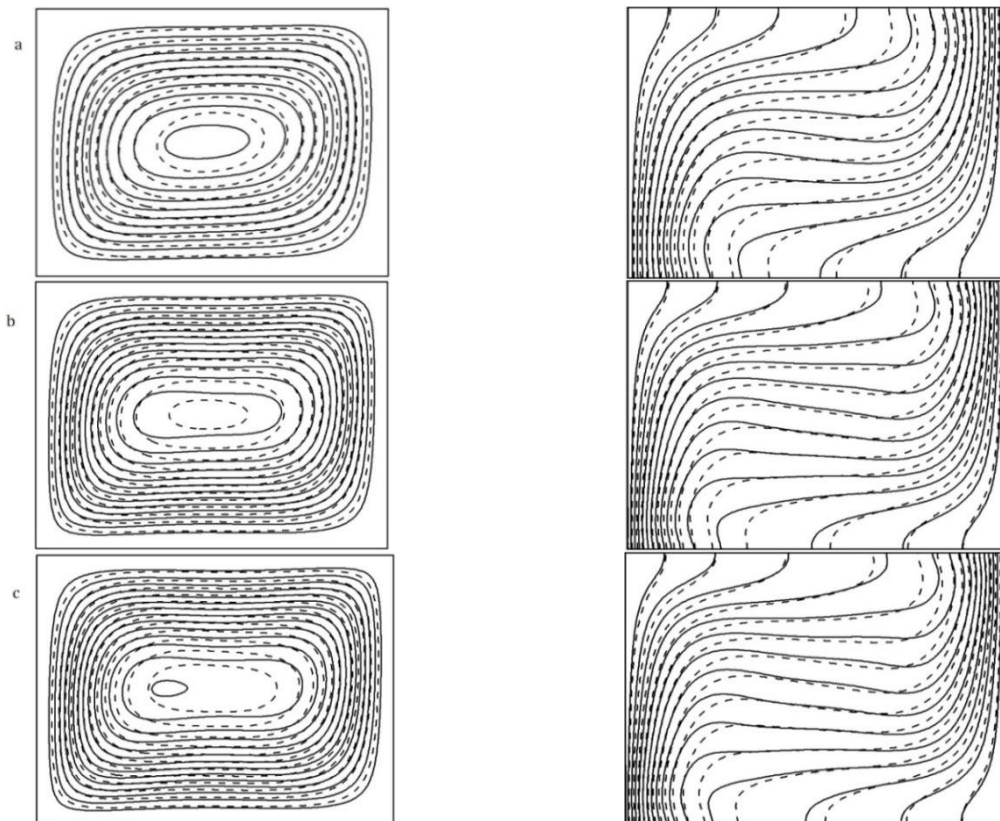


Figure 10. Comparison of the streamlines contours (left) and isotherms contours (right) for nanofluid at $Pr = 5.83$ (—) and nanofluid at $Pr = 3.42$ (---) for $\phi = 0.05$, $Gr = 10^4$, a) $dp = 24$ nm, b) $dp = 47$ nm, c) $dp = 100$ nm

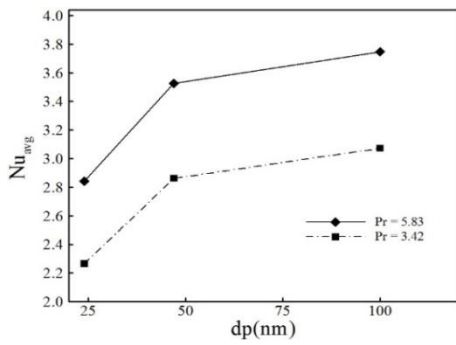


Figure 11. Variation of Nu with mean nanoparticle diameter for nanofluid with $\phi = 0.04$ and $Gr = 10^4$

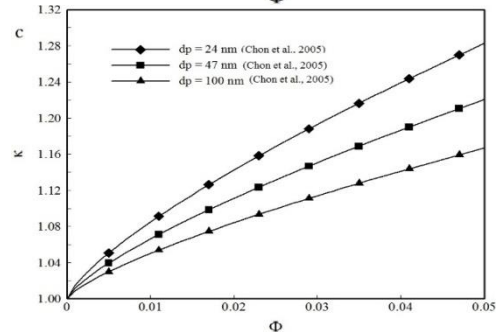
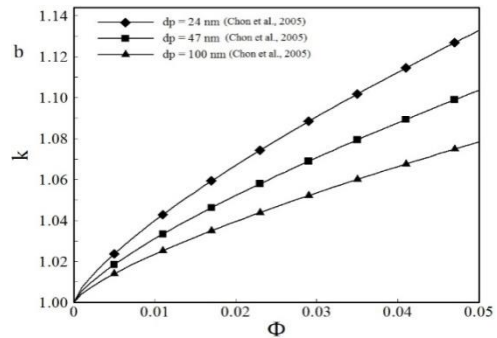
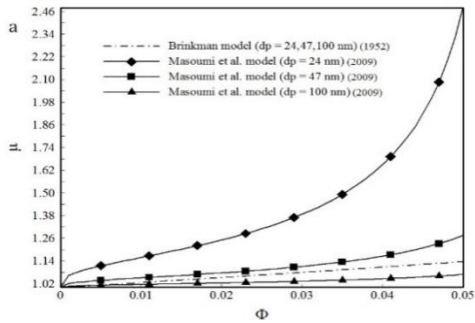


Figure 1. Comparison of the correlations used for the ratio dynamic viscosity and ratio thermal conductivity a,b) $Pr = 5.83$, c) $Pr = 3.42$

6. CONCLUSIONS

The lattice Boltzmann method is adapted to investigation of the influences of nanoparticles' mean diameter and temperature for the nanofluid free convection in a square cavity. This numerical analysis was performed for various values of parameters with results summarized as follows:

Increasing the nanoparticles have a substantially impact on the velocity and temperature of nanofluid. By adding nanoparticles, the vertical velocity decreases in the areas near the left wall of the enclosure while it increases in the neighborhood of cold wall in the enclosure. The rising of solid volume fraction reduces the Nusselt number. A similar behavior is found for decreasing the nanoparticles' mean diameter with addition of nanoparticles as well. A similar behavior is found for decreasing the nanoparticles' mean diameter with addition of nanoparticles as well. The same effect is observed through a decrease of nanoparticles' mean diameter and through an increase in nanoparticles concentration. It is found that the Nu_{avg} and absolute circulation strength increase with arise of the nanoparticles' mean diameter. It is obvious that the Nu_{avg} varies noticeable for different Prandtl numbers. For the Nu_{avg} , the variation of Prandtl number through the variation of the nanoparticles 'mean diameter has no significant affected.

7. REFERENCES

1. Abu-Nada, E., "Natural convection heat transfer simulation using energy conservative dissipative particle dynamics", *Physical Review E*, Vol. 81, No. 5, (2010), <https://doi.org/10.1103/PhysRevE.81.056704>.
2. Calcagni, B., Marsili, F. and Paroncini, M., "Natural convective heat transfer in square enclosures heated from below", *Applied Thermal Engineering*, Vol. 25, No. 16, (2005), 2522-2531.
3. Kuznik, F., Vareilles, J., Rusaouen, G. and Krauss, G., "A double-population lattice boltzmann method with non-uniform mesh for the simulation of natural convection in a square cavity", *International Journal of Heat and Fluid Flow*, Vol. 28, No. 5, (2007), 862-870.
4. Chol, S. and Estman, J., "Enhancing thermal conductivity of fluids with nanoparticles", *ASME-Publications-Fed*, Vol. 231, (1995), 99-106.
5. Ghadimi, A., Saidur, R. and Metselaar, H., "A review of nanofluid stability properties and characterization in stationary conditions", *International Journal of Heat and Mass Transfer*, Vol. 54, No. 17-18, (2011), 4051-4068.
6. Shahriari, A., Javaran, E.J. and Rahnama, M., "Effect of nanoparticles brownian motion and uniform sinusoidal roughness elements on natural convection in an enclosure", *Journal of Thermal Analysis and Calorimetry*, Vol. 131, No. 3, (2018), 2865-2884.
7. Ziaei-Rad, M., Saedan, M. and Afshari, E., "Simulation and prediction of mhd dissipative nanofluid flow on a permeable stretching surface using artificial neural network", *Applied Thermal Engineering*, Vol. 99, (2016), 373-382.
8. Ziaei-Rad, M., Kasaeipoor, A., Rashidi, M.M. and Lorenzini, G., "A similarity solution for mixed-convection boundary layer nanofluid flow on an inclined permeable surface", *Journal of Thermal Science and Engineering Applications*, Vol. 9, No. 2, (2017), doi: 10.1115/1.4035733.
9. Murshed, S., Leong, K. and Yang, C., "Thermophysical and electrokinetic properties of nanofluids—a critical review", *Applied Thermal Engineering*, Vol. 28, No. 17-18, (2008), 2109-2125.
10. Choi, S., Zhang, Z. and Keblinski, P., *Nanofluids, encyclopedia of nanoscience and nanotechnology (hs nalwa, editor)*, vol. 5. P.(757-773). 2004, American Scientific Publisher.
11. Khanafer, K., Vafai, K. and Lightstone, M., "Buoyancy-driven heat transfer enhancement in a two-dimensional enclosure utilizing nanofluids", *International Journal of Heat and Mass Transfer*, Vol. 46, No. 19, (2003), 3639-3653.
12. Putra, N., Roetzel, W. and Das, S.K., "Natural convection of nano-fluids", *Heat and Mass Transfer*, Vol. 39, No. 8-9, (2003), 775-784.
13. Wen, D. and Ding, Y., "Formulation of nanofluids for natural convective heat transfer applications", *International Journal of Heat and Fluid Flow*, Vol. 26, No. 6, (2005), 855-864.
14. Hwang, K.S., Lee, J.-H. and Jang, S.P., "Buoyancy-driven heat transfer of water-based Al_2O_3 nanofluids in a rectangular cavity", *International Journal of Heat and Mass Transfer*, Vol. 50, No. 19-20, (2007), 4003-4010.
15. Kim, J., Kang, Y.T. and Choi, C.K., "Analysis of convective instability and heat transfer characteristics of nanofluids", *Physics of Fluids*, Vol. 16, No. 7, (2004), 2395-2401.
16. Lin, K.C. and Violi, A., "Natural convection heat transfer of nanofluids in a vertical cavity: Effects of non-uniform particle diameter and temperature on thermal conductivity", *International Journal of Heat and Fluid Flow*, Vol. 31, No. 2, (2010), 236-245.
17. Jang, S.P., Lee, J.-H., Hwang, K.S. and Choi, S.U., "Particle concentration and tube size dependence of viscosities of Al_2O_3 -water nanofluids flowing through micro-and minitubes", *Applied Physics Letters*, Vol. 91, No. 24, (2007), <https://doi.org/10.1063/1.2824393>.
18. Xu, J., Yu, B., Zou, M. and Xu, P., "A new model for heat conduction of nanofluids based on fractal distributions of nanoparticles", *Journal of Physics D: Applied Physics*, Vol. 39, No. 20, (2006), 4486-4490.
19. Nguyen, C., Desgranges, F., Roy, G., Galanis, N., Maré, T., Boucher, S. and Mintsa, H.A., "Temperature and particle-size dependent viscosity data for water-based nanofluids—hysteresis phenomenon", *International Journal of Heat and Fluid Flow*, Vol. 28, No. 6, (2007), 1492-1506.
20. Li, J., Li, Z. and Wang, B., "Experimental viscosity measurements for copper oxide nanoparticle suspensions", *Tsinghua Science and Technology*, Vol. 7, No. 2, (2002), 198-201.
21. Masoumi, N., Sohrabi, N. and Behzadmehr, A., "A new model for calculating the effective viscosity of nanofluids", *Journal of Physics D: Applied Physics*, Vol. 42, No. 5, (2009), <https://doi.org/10.1088/0022-3727/42/5/055501>.
22. Chon, C.H., Kihm, K.D., Lee, S.P. and Choi, S.U., "Empirical correlation finding the role of temperature and particle size for nanofluid (Al_2O_3) thermal conductivity enhancement", *Applied Physics Letters*, Vol. 87, No. 15, (2005), <https://doi.org/10.1063/1.2093936>.
23. Kao, P.-H. and Yang, R.-J., "Simulating oscillatory flows in rayleigh–benard convection using the lattice boltzmann method", *International Journal of Heat and Mass Transfer*, Vol. 50, No. 17-18, (2007), 3315-3328.

24. Brinkman, H., "The viscosity of concentrated suspensions and solutions", *The Journal of Chemical Physics*, Vol. 20, No. 4, (1952), 571-571.
25. Fox, R.W., McDonald, A.T. and Pritchard, P.J., "Introduction to fluid mechanics 6th edition, John Wiley & Sons", Wiley, New York, (2004).

Assessment of Particle-size and Temperature Effect of Nanofluid on Heat Transfer Adopting Lattice Boltzmann Model

A. Shahriari^a, N. Jahantigh^a, F. Rakani^b

^a Department of Mechanical Engineering, University of Zabol, Zabol, Iran

^b Department of Computer Sciences, University of Sistan & Baluchestan, Zahedan, Iran

P A P E R I N F O

چکیده

Paper history:

Received 18 November 2017

Received in revised form 08 December 2017

Accepted 05 February 2018

Keywords:

Nanoparticles Mean Diameter

Natural Convection

Nanofluid

Lattice Boltzmann Model

هدف مطالعه حاضر بررسی اثرات قطر متوسط نانوذرات و دمای نانوسیالآبی اکسید آلومینیم (Al_2O_3) بر روی میدان سرعت و توزیع دما با استفاده از روش شبکه بولتزمن است. دیواره‌های سمت راست و چپ محفظه به ترتیب در دمای گرم و سرد قرار دارند در حالی که دیواره بالا و پایین هر دو صاف عایق شده‌اند. اثر پارامترهایی نظیر عدد گراشف ($Gr=10^3, 10^4, 10^5$) عدد پرانتل ($Pr=3.42, 5.83$)، کسر حجمی نانوذرات ($\phi = 0, 0.01, 0.03, 0.05$) اندازه ذرات ($dp=24, 47, 100$ nm) بر روی میدان جریان و میدان دما مطالعه شده است. می‌توان نتیجه گرفت که میدان-های جریان و توزیع دما متأثر از اضافه شدن نانوذرات می‌باشند. با افزایش کسر حجمی نانوذرات انتقال حرارت کاهش می‌یابد؛ با این حال با افزایش عدد گراشف و قطر متوسط نانوذرات مشاهده می‌شود که انتقال حرارت افزایش می‌یابد. کاهش قطر متوسط نانوذرات و عدد پرانتل اثر مشابهی بر روی عدد ناسلت دارند. هم‌چنین مشاهده شد که عدد ناسلت میانگین نسبت به مدل هدایت حرارتی حساسیت کمتری نسبت به مدل ویسکوزیته دینامیکی دارد.

doi: 10.5829/ije.2018.31.10a.18